

Research on Hydrodynamic Interaction between Multiple Floating Bodies

Y.Gou & B. Teng

State Key Laboratory of Coastal and Offshore Engineering, Dalian University of Technology, Dalian, Liaoning Province, China

ABSTRACT: The hydrodynamic interaction between the multi-bodies can not be neglected when bodies are closed to each other. In this paper the diffraction and the radiation problems of multiple floating bodies are considered by the higher-order boundary element method (HOBEM). To improve the efficiency of HOBEM for large scale computation, a fast multipole method is applied, in which a direct method is used to compute the free-term coefficient and the Cauchy principal value (CPV) integral. Using the present numerical model, the hydrodynamic coefficients and the exciting forces of three parallel wiggly ships are studied in this paper. Numerical experiments are carried out to examine the effect of the distance between the ships, the number of the ships and the incident wave frequency. By comparison with the results of a single ship in the open sea, it is found the hydrodynamic coefficients and exciting forces are significantly different.

1 INTRODUCTION

Multiple-body structures are widely used in coastal and offshore engineering exploration. The hydrodynamic interaction between the multi-bodies must be considered in some cases, such as the structures supported by a array of columns, floating bridges and so on. The problem of multiple bodies was studied by Ohkusu (1969) firstly. In his research, the hydrodynamic interactions between two cylinders were considered.

The linear potential theory still suits the problems of the wave and multiple floating bodies (Newman, 2001). The methods which used for single body can be extended to multiple bodies, such as the eigenfunction expansions method (Ohkusu, 1972), the panel method (***, 19**), and the HOBEM (Eatock Taylor and Chau, 1991; Teng and Eatock Taylor, 1995). For an arbitrary structure the HOBEM is powerful. In HOBEM the surface of structures can be discretized by curve elements, and it keep the continuous of potential and its derivative at element nodes. So it will obtain more accurate results with fewer elements. However, HOBEM is still a method with N^2 (N is the number of unknowns) storage and computation cost. For multi-bodies problems, fully consideration of the hydrodynamic interaction between multi-bodies is often beyond computer's ability. In this paper a highly efficient method, the fast multipole accelerated higher order boundary method (FMM) (Teng and Gou, 2006), is used to the hydrodynamic interaction between multi-bodies. Three wiggly ships is used for as an example, and numerical computations are carried out to examine the effect due to the distance between two ships, number of the ships and the incident wave frequency.

2 FORMULATIONS

Potential flow is assumed. Time-harmonic motions of small amplitude are considered, and then all the time-dependent quantities can be separated. The velocity potential ϕ satisfies the Laplace equation and the following boundary conditions:

$$\nabla^2 \phi = 0 \quad (1)$$

$$\frac{\partial \phi(\mathbf{x})}{\partial z} = \frac{\omega^2}{g} \phi(\mathbf{x}) \quad \text{on } S_F \quad (2)$$

$$\frac{\partial \phi(\mathbf{x})}{\partial z} = 0 \quad \text{on } S_D \quad (3)$$

$$\frac{\partial \phi(\mathbf{x})}{\partial n} = V_n \quad \text{on } S_B \quad (4)$$

where S_F , S_D , S_B represent the free surface, the sea bottom and the body surface respectively. V_n is the normal velocity on the body surface. The scattering velocity potential satisfies the radiation condition at infinity. The velocity potential can be decomposed into three components:

$$\phi = \phi_i + \phi_d + \phi_r \quad (5)$$

where ϕ_i is the velocity potential of the incident waves, ϕ_d the diffraction potential, ϕ_r the radiation potential. For a single floating body, it has six degrees of freedom: surge, sway, heave, roll, pitch and yaw. For M bodies, the definition of the radiation potential is the extension of the single body theory. Thus ϕ_r can be represented as the sum of unit radiation potential in the six directions of all bodies

$$\phi_r = \sum_{j=1}^{6 \times M} -i\omega \xi_j \phi_j \quad (6)$$

where ϕ_j ($j=1, \dots, 6M$) is the unit radiation potential induced by one body motion in a single direction, ξ_j ($j=1, \dots, 6M$) is the complex amplitude of the corresponding rigid body motion.

Substituting Eq. (5) into the body surface boundary condition, Eq. (4), we obtain:

$$\frac{\partial \phi_d}{\partial n} = -\frac{\partial \phi_i}{\partial n} \quad \frac{\partial \phi_j}{\partial n} = n_j \quad (7)$$

where n_j ($j=1, \dots, 6M$) the normal derivative of the j th degree of freedom:

$$n_j = \begin{cases} 0 & j \neq 6(m-1)+1, \dots, 6m \\ n^m & j = 6(m-1)+1, \dots, 6m \end{cases} \quad (8)$$

where n^m is the m th body's six normal derivative.

Putting the source point on the body surface, and applying the second Green's theorem to Green function and velocity potential ϕ_j and ϕ_d , we can obtain the integral equation:

$$\alpha \phi(\mathbf{x}_0) - \iint_{S_B} \frac{\partial G(\mathbf{x}, \mathbf{x}_0)}{\partial \mathbf{n}} \phi(\mathbf{x}) \, ds = - \iint_{S_B} \frac{\partial \phi(\mathbf{x})}{\partial \mathbf{n}} G(\mathbf{x}, \mathbf{x}_0) \, ds \quad (9)$$

where α is so called as the free-term coefficient or the solid angle coefficient. The Green function G satisfies the linear free-surface boundary condition, the radiation condition at infinity and the impermeable condition on the seabed. Combining the integral equation outside the body with another one inside the body, Eatock Taylor and Chau (1991) derived a new equation without the solid angle, but with an integral on the inner free surface. Teng and Eatock Taylor (1995) removed the integral on the inner water plane by taking a new Green function used in the integral equation inside the body. Those methods are called as the indirect methods for computing the free-term coefficient. By discretizing the body surface into higher-order elements and transforming them into isoparametric elements, the numerical integral can be resolved.

Thus, the diffraction and unit radiation potential can be obtained, and then we can get the added mass and damping coefficients.

The coefficient matrix of the boundary element method is full. Both the operation count and the memory requirements for the matrix equation setup are of the order $O(N^2)$, where N is the number of unknowns. For the multi-body cases in sea structures, size of the bodies is bigish, so the number of unknowns is very large. And huge computer resources are required for storage and computation. In this paper, FMM is used to improve the compute efficiency and decrease the storage memory. In this method, when the field point is far from the source point, the Green function in series form which satisfied the free surface boundary condition can be expanded in the cylindrical coordinate system by Graf's addition theorem, and calculated approximately, it needn't to form the coefficient matrix of the Eq. (9) (Utsunomiya, Watanabe et al. 2001; Utsunomiya and Watanabe, 2002). The operation count and the memory requirements reduce from $O(N^2)$ to $O(N)$ in this method. However, all those indirect method for computing the free-term coefficient α will increase the compute effort. In this paper a geometrical method (Mantic, 1993) is used to get α directly, and a direct method is implemented for computing the double layer CPV integral in the integral equation (Guiggiani, 1990).

3 NUMERICAL EXAMPLES

In this paper, three wigley ships are taken as an example to examine the interactions of the multiple ships. The surface of each wigley ship satisfies the formula:

$$y = b[1 - (\frac{2x}{a})^2][1 - (\frac{z}{T})^2] \quad (10)$$

where (x, y, z) is the coordinate of the ship surface, $b=B/2$ the half breath of the ship, B the ship breath, a the ship length, T the ship draft. The definition of the coordinate system is showed in Fig. 1, and the locations of the three ships are shown in Fig. 2.

In the computation, $a=100\text{m}$, $b/a=0.05$, $T/a=0.0625$. The water depth $h=30\text{m}$. The incident waves propagate from the negative x direction. The wet surface of each ship is discretized with 1040 higher-order elements, 52 longitudinal subdivisions and 10 vertical subdivisions.

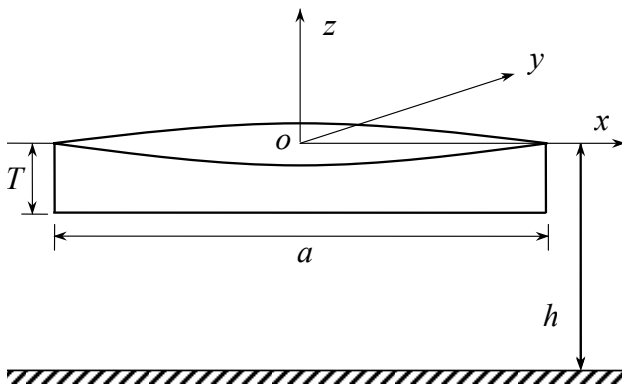


Fig.1 Definition of the coordinates

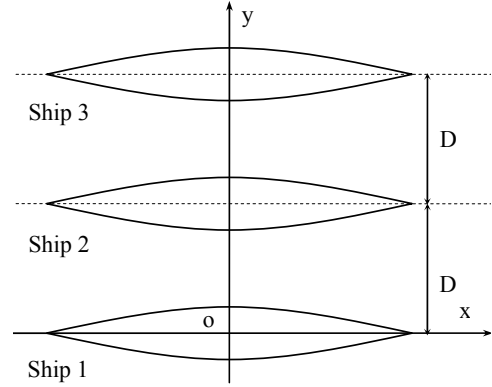


Fig.2 Sketch of the locations of three ships

3.1 The results of Ship 1 in three conditions

In this section we will research the hydrodynamic interaction between Ship 1 and the other ships. Three conditions are considered: single ship means only Ship 1 is in existence, double ships means Ship 1 and Ship 2 are in existence together, and triple ships means the three ships are all located as shown in Fig. 2. The distance D between two ships equals to 20m. The results

of hydrodynamic coefficient of Ship 1 are shown in Fig. 3. Because they have analogical characteristic, only some results are shown here. The subscripts of the hydrodynamic coefficients are corresponding to the generalized normal direction of body motion respectively. Fig. 4 shows the exciting force on Ship 1. The incident wave angle is 90 degree. That means that waves are incident along the positive y direction.

From Fig. 3 it can be seen that the influence of the existence of Ship 2 and Ship 3 is small at the low wave frequency domain, but it is significant at the high frequency domain. The results of Ship1 are smooth when only Ship1 is in existence. However, when the other ships are located, the results are fluctuant at the high wave frequency domain. The fluctuation is more obvious when the three ships are in existence together. The influence on the exciting force on Ship1 is significant too. The influence is not only in the high frequency domain, but also in the low frequency domain, we can see it from Fig. 4 (b).

3.2 *The results of three parallel ships*

In this section we consider the hydrodynamic coefficient and exciting force on each ship when three ships are located together as shown in Fig. 2. The distance D between two ships still equals to 20m. Fig. 5 shows the results of some hydrodynamic coefficients. It is obvious that the hydrodynamic results of Ship 1 are the same with those of Ship 3, so only the results of Ship 1 and Ship 2 are shown in Fig. 5. Fig. 6 shows the exciting force on the three ships. The incident waves propagate along the positive y direction.

From Fig. 5 we can see that the peak value appears on Ship 2. The results of Ship 1 are close to those of Ship 2 in the low frequency domain, but in the high frequency domain the peak value of Ship 2 is almost twice as those of Ship 1. The exciting forces on the three ships are shown in Fig. 6. From Fig. 6 (a) and (c) we can draw the similar conclusion that the results have great difference at the high frequency domain, and the largest value appears on Ship 2. But Fig. 6 (b) shows that the influence among ships is significant in most frequency range and the value on Ship 1 is mostly larger than that on Ship 2.

3.3 *The influence of the distance between two ships*

In this section the distance between two ships has been changed. Three distances are chose to do the examination, 20m, 30m and 40m. The computation domain of ka is from 0 to 16. The results shown in Fig. 7 are the hydrodynamics coefficient of Ship 1. All the results have the same character, so that only two of them are plotted. The solid curve is the results of only Ship 1. Through the comparison between the curves, we can see that with the increase of the distance between ships the peak value frequency moves to low frequency and the value decreases. But if we choose one frequency, it can be seen that the value is not always decreasing with the increase of the distance.

Fig. 8 shows the influence of the distance between ships on the hydrodynamic coefficients at $ka=11$. The distance between two ships is nondimensioned by the wave length. From Fig. 8 it can be seen that the value is correlative with the ratio of the distance to the wave length. The hydrodynamic coefficients oscillate with the increase of the distance, and the oscillating period is the half of the dimensionless distance.

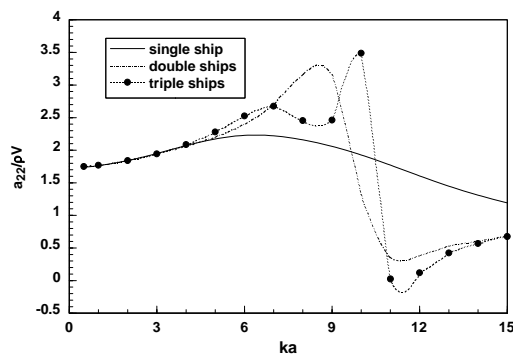
4 CONCLUSIONS

In this paper a fast multipole accelerated higher-order boundary element method is used to study the hydrodynamic interaction among multiple floating bodies. Three parallel wiggly ships are applied in the examination. From the numerical results the some conclusions can be drawn:

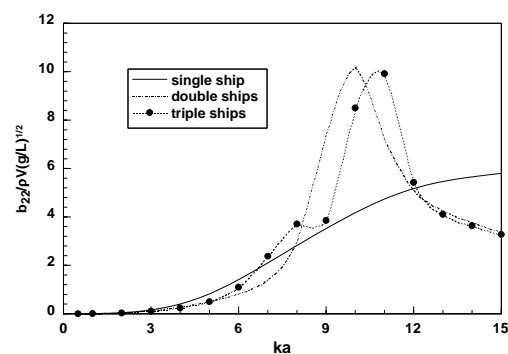
1. The influence due to the other ships is significant on the results of hydrodynamic coefficients and the exciting force at the high frequency domain. For heave exciting force, even at the low frequency domain the interaction is still significant.
2. When the three ships parallel each other, the peak value of the hydrodynamic coefficients and exciting force appear on the middle ship, except the heave exciting force. The results of each ship are almost the same in the low frequency domain except the heave exciting force.
3. For two parallel ships, the hydrodynamic coefficients oscillate with the increase of the distance, and the oscillating period is the half of the ratio of the distance between ships and the wave length.

REFERENCE

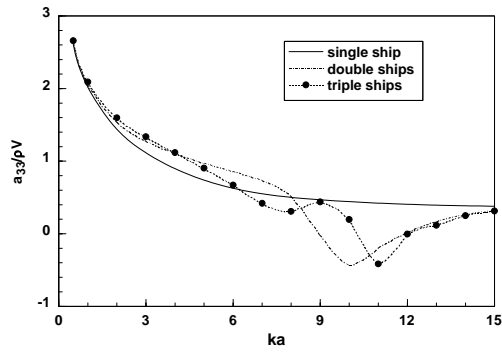
- Eatock Taylor, R., Chau F P 1991. Wave diffraction theory-some developments in linear and non-linear theory. *Proc. of OMAE* 1: 19-27
- Guiggiani, M. and Gigante, A. 1990. A general algorithm for multidimensional Cauchy Principal Value Integrals in the boundary element method *Journal of Applied Mechanics*, 57: 906-915.
- Mantic, V. 1993. New formula for the C-matrix in the Somigliana identity. *Journal of Elasticity*, 33(3): 191-201
- Newman J N. 2001. Wave effects on multiple bodies. *Hydrodynamics in Ship and Ocean Engineering*, 3-26.
- Ohkusu M. 1969. On the heaving motion of two circular cylinders on the surface of a fluid. *Reports of Research Institute for Applied Mechanics*, XVII, 58: 167-185.
- Ohkusu M. 1972. Wave action on groups of vertical circular cylinders (in Japanese). *J. Society of Naval Architects of Japan*, 131: 53-64
- Utsunomiya, T. and Watanabe, E. 2002. Accelerated Higher Order Boundary Element Method for Wave Diffraction/Radiation Problems and Its Applications. *Proc. 12th Int.Offshore and Polar Eng. Conf.*, 305-312.
- Utsunomiya, T., Watanabe, E. et al. 2001. Fast multipole algorithm for wave diffraction/radiation problems and its application to VLFS in variable water depth and topography. *Proc. of OMAE* 01-5202, 321-327
- Teng, B. and Eatock Taylor, R. 1995. New higher-order boundary element methods for wave diffraction/radiation. *Applied Ocean Research*, 17(2): 71-77
- Teng, B. and Gou, Y. 2006. Fast Multipole Expansion Method and Its Application in BEM for Wave Diffraction and Radiation. *Proc. 16th Int.Offshore and Polar Eng. Conf.*, 3: 318-325



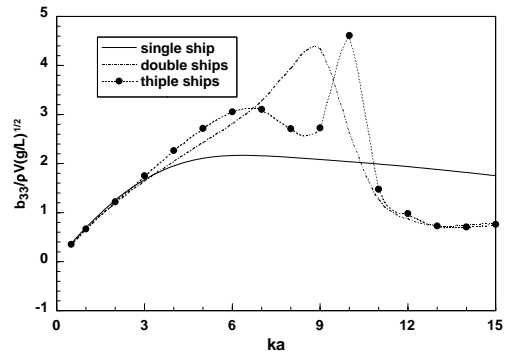
(a) a22



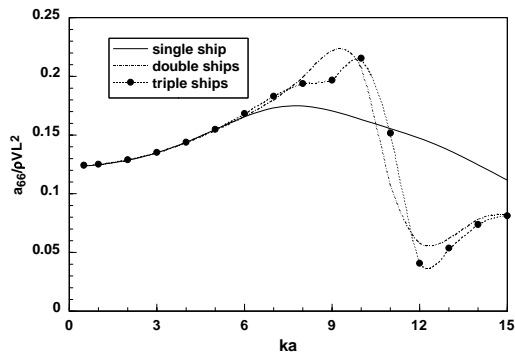
(b) b22



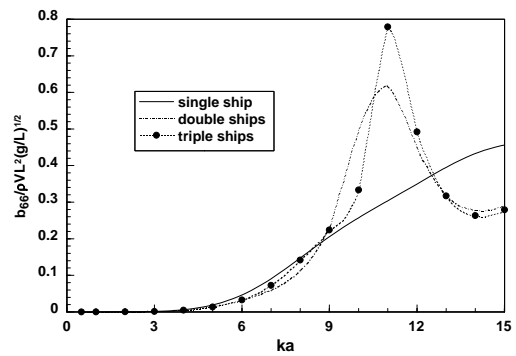
(c) a_{33}



(d) b_{33}

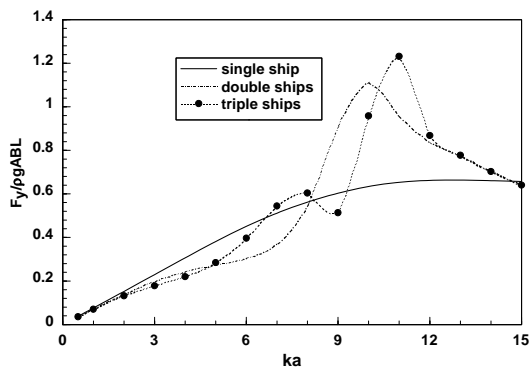


(e) a_{66}

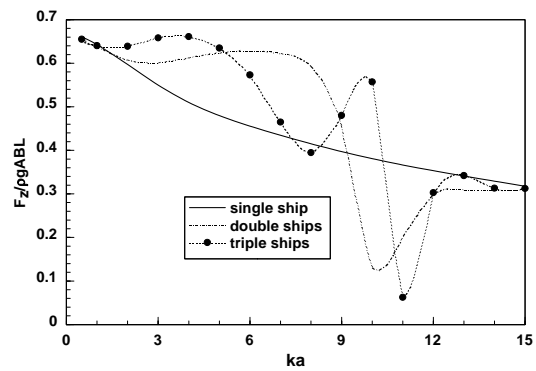


(f) b_{66}

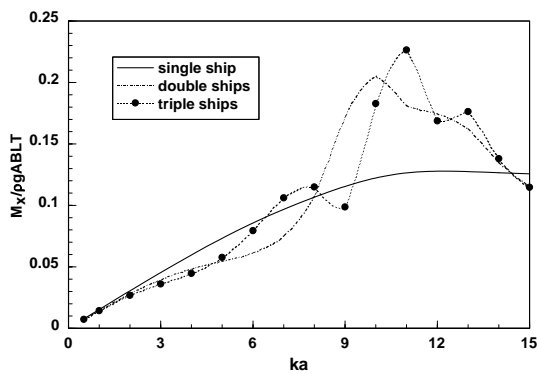
Fig. 3 Hydrodynamic coefficient of ship1 in three conditions



(a) F_y

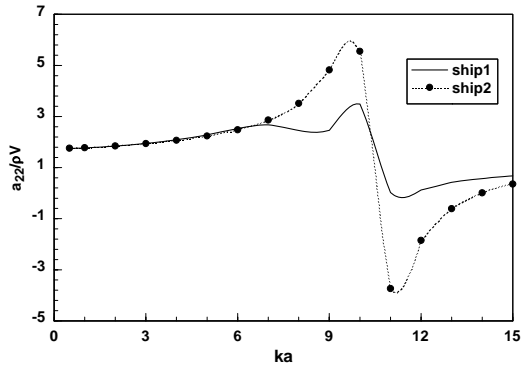


(b) F_z

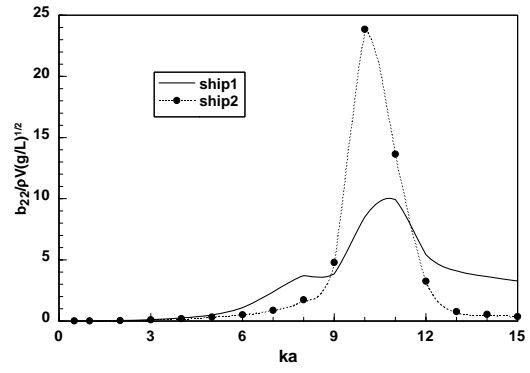


(c) M_x

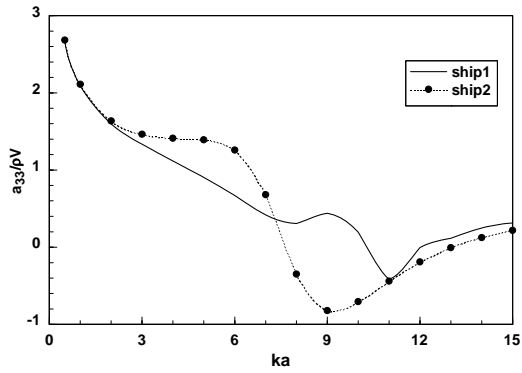
Fig. 4 Exciting force of ship1 in three conditions



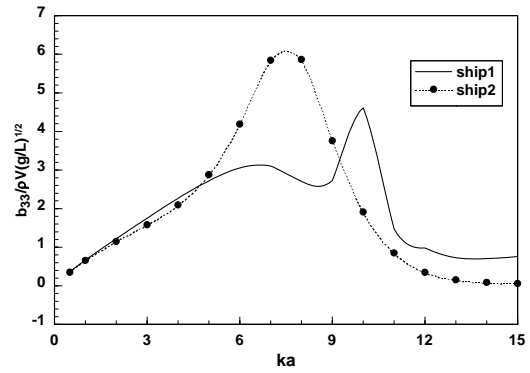
(a) a_{22}



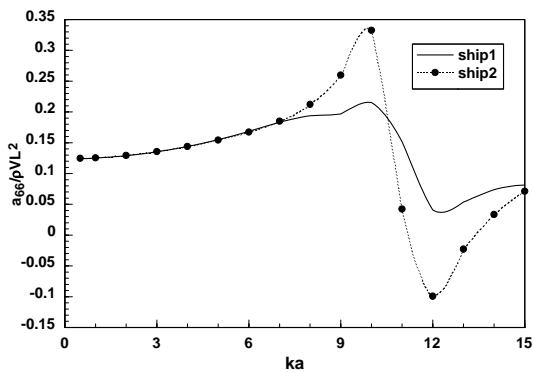
(b) b_{22}



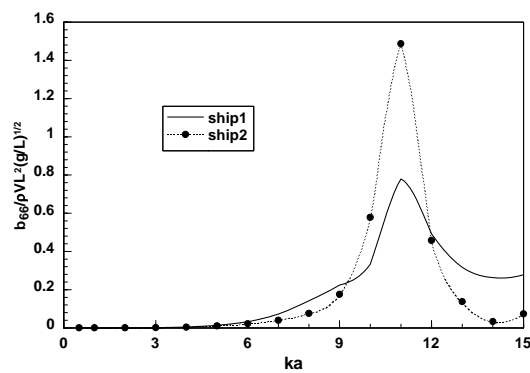
(c) a_{33}



(d) b_{33}

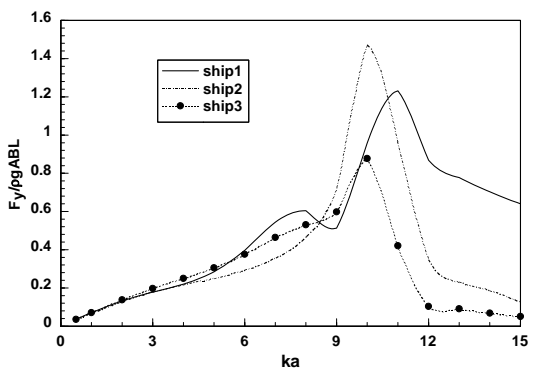


(e) a_{66}

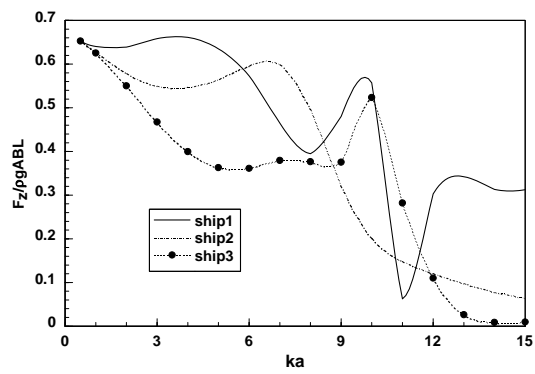


(f) b_{66}

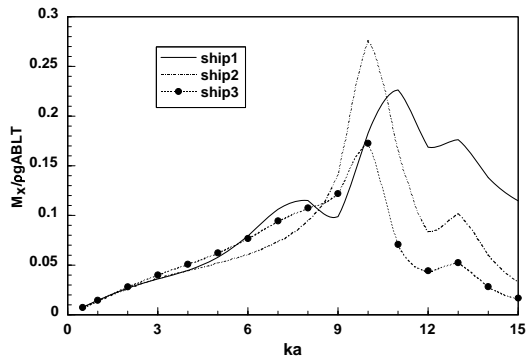
Fig. 5 Hydrodynamic coefficients of ship1 and ship2



(a) F_y

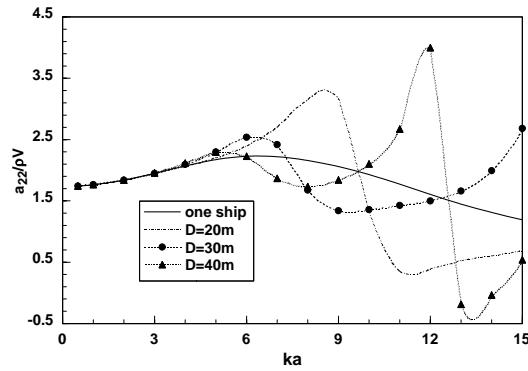


(b) F_z

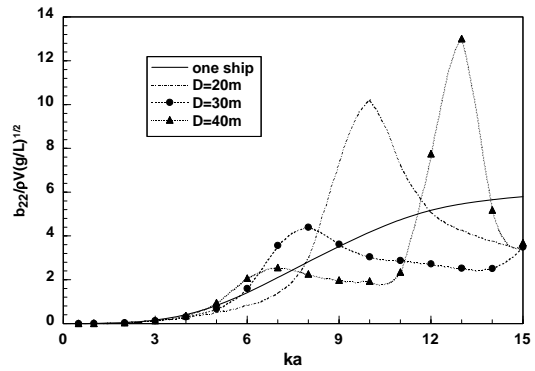


(c) M_x

Fig. 6 Results of exciting force on three ships

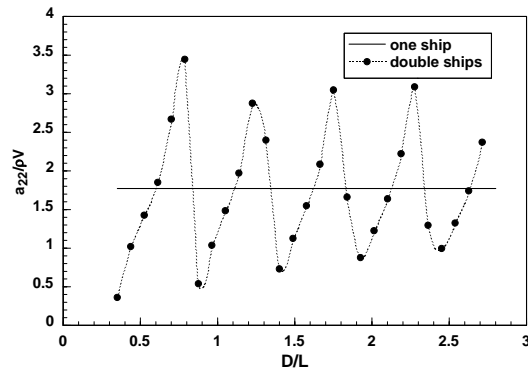


(a) a_{22}

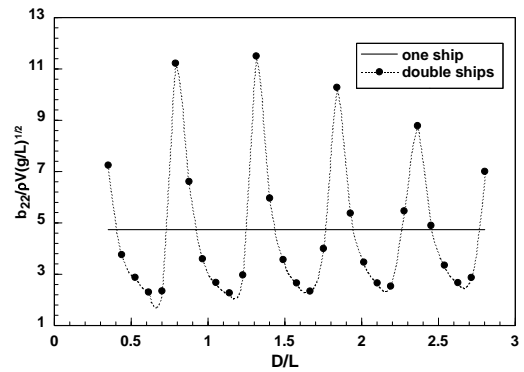


(b) b_{22}

Fig. 7 Hydrodynamic coefficients of ship1 with different D from ship2



(c) a_{22}



(d) b_{22}

Fig. 8 Hydrodynamic coefficients of ship1 with different D at $ka=11$